EUROFUSION WPJET1-PR(16) 16451

L Piron et al.

Plasma stability in advanced JET ITER-like wall plasmas: first measurements and modelling

Preprint of Paper to be submitted for publication in Nuclear Fusion

This work has been carried out within the framework of the EUROfusion Consortium and has received funding from the Euratom research and training programme 2014-2018 under grant agreement No 633053. The views and opinions expressed herein do not necessarily reflect those of the European Commission.

Plasma stability in advanced JET ITER-like wall plasmas: first measurements and modelling

L. Piron[1], E. Alessi[2], Y.Q. Liu[1], M.P. Gryaznevich[1], M. Baruzzo[3], D. Alves[4], P. Buratti[5], N. Hawkes[1], T.C. Hender[1], I. Lupelli[1], J. Mailloux[1] and JET contributors*
[1] *EUROfusion Consortium, JET, Culham Science Centre, Abingdon, OX14 3DB, UK*
[2] *Istituto di Fisica del Plasma, C.N.R., EURATOM-ENEA Association, Milan, Italy*
[3] *Consorzio RFX, EURATOM-ENEA Association, Corso Stati Uniti 4, 35127 Padova, Italy*
[4] *European Organization for Nuclear Research, CERN, F-01631 CERN Cedex, France*
[5] *C.R. ENEA Frascati, via E. Fermi 45, 00044 Frascati, Italy*
(*) *See the appendix of Romanelli F. et al 2014 Proc. 25th IAEA Fusion Energy Conf. 2014 (Saint Petersburg, Russia, 2014).*
(Dated: October 17, 2016)

Abstract Advanced tokamak plasma operations are associated with increased normalized beta and are often limited by pressure-driven MHD instabilities. A conducting wall has a beneficial effect increasing the beta limit, however, the ideal no-wall beta-limit as set by the resistive wall mode (RWM) has often been a major obstacle to such operations. The plasma stability has been investigated recently in JET ITER-like wall (ILW) advanced tokamak plasmas by applying magnetic field perturbations using external non-axisymmetric coils (EFCCs), probing the plasma for its response. The study presented here investigates the differences of magnetic field penetration and plasma stability due to the change from the JET-Carbon (C) wall to the ILW both experimentally and through MARS-F code predictions. A reduction of the beta limit reached in ILW plasmas, of about 12%, has been observed and the physics of the beta collapse has changed with respect to the C wall one. These differences are not caused by the change of the resistive properties of the wall, since the wall frequency response in vacuum is unaltered, but they can be associated to a change of the plasma pressure profile.

I. INTRODUCTION

Stability at high plasma pressure is an important requisite for advanced tokamak scenarios, such as those foreseen for ITER and compatible with the steady-state operation of future reactors [1]. Such scenarios rely on increased normalised beta (β_N) plasmas for efficient operation. β_N is defined as $\beta_N = \beta B_t a/I_p$, where β is the ratio of the plasma pressure to the magnetic field pressure, B_t the toroidal magnetic field, a the minor radius a and I_p the plasma current. As reported in [2], the resistive wall mode (RWM), which is a global kink-like, non-axisymmetric instability, has often been considered as a major obstacle to steady state operation of advanced tokamaks. Although the presence of a conducting first wall tends to increase the β-limit, it is critical to ensure that the RWM stays stable when the plasma pressure exceeds the ideal no-wall beta limit, $\beta_N^{no-wall}$, which is the limit in the absence of the stabilising influence of surrounding wall [3].

A safe way of probing no-wall stability consists of examining the plasma response to externally applied magnetic fields. When the plasma pressure exceeds the no-wall β limit, an enhancement of the plasma response often referred to as Resonant Field Amplification (RFA), occurs. In particular, the RFA is defined as the ratio of the plasma response to the externally applied magnetic field.

Looking for the RFA enhancement as means for the no-wall limit has been used in scenario development of high-β experiments in several devices, such as DIII-D [4–6], JET [7, 8, 10–12] and ASDEX Upgrade [13] tokamaks and in RFX-mod reversed-field pinch [14]. In particular, in JET-Carbon (C) wall plasmas, the plasma response to externally applied rotating magnetic fields has been also observed to increase before the destabilization of a fast rotating internal kink or tearing mode and at lower β, during ELM-free H-mode periods and before the appearance of the first type-I ELM, as described in [11].

Recently, the JET-C wall has been replaced by an ITER-like wall (ILW), composed of beryllium for the main chamber wall and Tungsten in the divertor. In this work, the first measurements of RFA in advanced scenarios in JET-ILW plasmas are presented and compared with the results obtained in JET-C wall plasmas. The plasma stability limit so identified has been compared also with MARS-F code predictions [15].

The manuscript is structured as followed: in section 2 the frequency response of JET wall to magnetic field perturbations induced by EFCC is characterized. This study is important to understand if the change of JET wall has an impact on the magnetic field penetration. In section 3 the first measurements of RFA in ILW plasmas are presented in both high and low beta regimes and the main results obtained are compared with Carbon ones. The stability limit experimentally identified is compared with MARS-F code stability results. The summary and conclusions of this work are given in section 4.

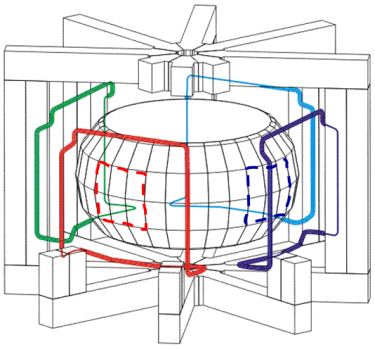

Figure 1: Position of the external error field correction coils (solid colored lines) and the corresponding saddle loops sensors (dashed lines) on JET.

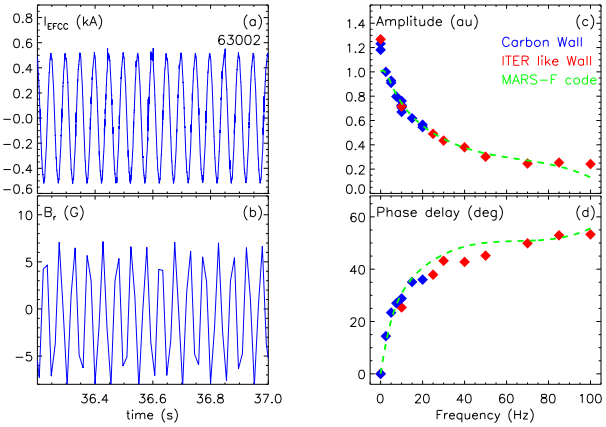

Figure 2: Time behaviour of (a) EFCC current and (b) n=1 magnetic field as measured by a combination of signals of midplane saddle loops located in the same octants as the EFCCs. (c-d) Transfer function between the EFCCs and n=1 connected saddle coils identified using JET-C (blue dots) and ILW data (red dots). The dashed green line corresponds to MARS-F code modelling.

II. FREQUENCY RESPONSE OF JET WALL

In the JET tokamak, external non-axisymmetric magnetic fields used to probe plasma stability can be applied using the EFCCs, which consist of four coils, spanning each 70° in toroidal angle, arranged symmetrically around the vacuum vessel and external to it [16]. The coils are located in octants $1, 3, 5$ and 7 of the vessel and an odd-n spectrum can be induced by feeding them with oppositely directed currents when toroidally opposite coils are connected. This is the coil configuration that has been used in the experiments analysed here. The response of the plasma to magnetic field perturbations can be measured using a toroidal array of saddle loops, which are mounted on the low field side midplane of the vacuum vessel. A sketch of EFCCs and saddle loops sensors of JET experiment is shown in Fig. 1.

The frequency response of the JET wall to externally applied magnetic fields perturbations in absence of plasma has been measured. This analysis is of fundamental importance in order to understand if the change of the JET wall can affect the magnetic field penetration, and so the eddy currents pattern in the first wall.

An example of JET-C experiment in vacuum is reported in Fig. 2(a-b), where the time behaviour of EFCC current rotating at 30Hz is shown in the top panel and the induced n=1 magnetic field, in the bottom one, as measured by a combination of midplane saddle loops signals located in the same octants as the EFCCs. Several vacuum shots with magnetic field perturbations rotating at frequency up to $100Hz$ have been analysed. In this way, the transfer function between EFCCs and midplane saddle loops can be calculated. The transfer function experimentally identified is reported in Fig. 2(c-d), where the blue symbols correspond to C wall data, the red ones to ILW. The data from the two ensembles of vacuum experiments match well, therefore it is possible to conclude that the penetration of the external magnetic field is not sensitive to the change of wall material in JET device.

The MARS-F code, which has been used for plasma stability studies, has been benchmarked against these data. In order to obtain a good match, a model with 2 shells has been implemented in the code. The first shell corresponds to the JET vacuum vessel, located at $r/a = 1.3$. Instead, the second one to a thin shell placed at $r/a = 1.7$, with a poloidal gap covering about 10% of the total poloidal circumference, and with the wall time 10 times larger than the JET wall time. The resistivity in such gap has been increased by a factor 100 with respect to the other region. The position of the second shell approximately corresponds to the location of the JET mechanical support structure. The fit achieved with this double shell model is reported in Fig. 2(c-d) with a dashed green line.

III. RESONANT FIELD AMPLIFICATION: MEASUREMENTS AND MODELLING

First measurements of RFA have been performed in JET-ILW in advanced tokamak scenarios. The time evolution of the main plasma parameters, i.e. plasma current, NBI power, D_α and β_N, for one of these experiments is reported in Fig. 3(a-c). The MHD activity, i.e. amplitude and frequency of several modes, is shown in Fig. 3(d-e). In this experiment, a $200A$ current oscillating at $30Hz$ has been applied to EFCCs connected in n=1 configuration, as show in Fig. 3(f). The induced magnetic field perturbation was typically 5 times below the locked mode onset error field threshold and was not seen by any other diagnostics except magnetics. By taking the ratio between the plasma response and the external magnetic field, the RFA indicator has been calculated. The plasma response has been measured by a n=1 combination of saddle coils located in octants orthogonal to

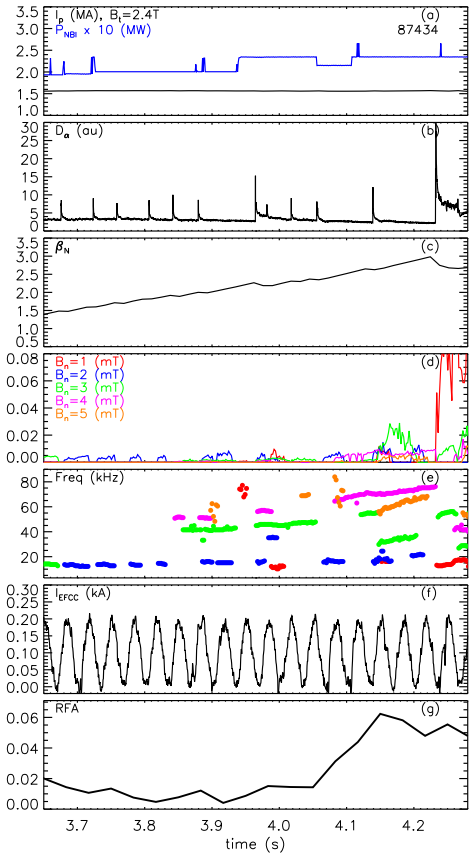

Figure 3: Time behaviour of (a) plasma current and NBI power, (b) D_α, (c) β_N, (d-e) amplitude and frequency of several modes, (f) current in EFCCs and (g) RFA measurement for 87434 JET-ILW plasma.

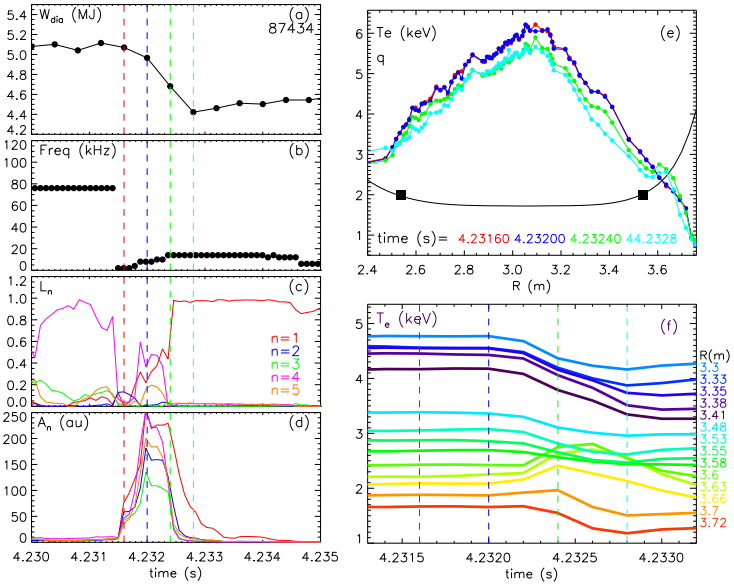

Figure 4: Time behavior of (a) diamagnetic plasma stored energy, (b) to (d) dominant mode frequency, n order number and amplitudes of modes before the beta collapse event from SVD analysis, (e) radial profiles of electron temperature from ECE measurements and q, and (f) time behaviour of electron temperature from different radial location. The squared markers correspond to the q=2 rational surface. The vertical dashed lines coincide with to the time instants of temperature radial profiles, shown in panel (e). The data corresponds to the same plasma experiment reported in Fig.3.

the EFCCs. Conversely, the external magnetic field has been evaluated at the EFCCs position. The behaviour of RFA as a function of time is reported in Fig.3(g). The response of the plasma is significantly enhanced when β_N is around 2.3. The sharp increase of RFA, by a factor 3, indicates that the plasma is near the no wall beta limit.

After the increase of RFA and in concomitance of a giant ELM, around $t = 44.2s$, a β collapse event happens, as shown in Fig. 3(c). Magnetic crashes associated with β collapses are very fast events, with durations of the order of $\approx 0.5ms$, and in this case the sudden loss of diamagnetic stored energy is about 10%. The time behavior of diamagnetic stored energy is reported in Fig. 4(a). The event in fact is mainly associated with a degradation of electron and ion temperature profiles as measured by Electron Cyclotron Emission (ECE) radiometer and Charge Exchange spectroscopy, respectively, within $R = 3.6m$.

In C wall plasmas, beta collapses affected a larger fraction of the plasma volume and were triggered by a global $n = 1$ kink-like MHD mode, as described in [23]. In the experiment analyzed here, since no global $n = 1$ kink-like activity has been observed before the beta collapse event, the Singular Value Decomposition (SVD) method [20] has been applied to Mirnov coil magnetic measurements in order to identify the MHD modes responsible of such event.

The SVD technique decomposes the input matrix X, the magnetic signals, in three matrices U, S, and V. Under the assumptions that data describes travelling sinusoidal waves along the toroidal direction, SVD is meant to be capable of discerning the different sinusoidal contributions from one another and from the noise. The columns of the U matrix will give information about the spatial periodicity of a mode, i.e. the toroidal order number, and are called as the Principal Axes (PA) of the mode. Instead, the rows of the V matrix will contain information about the temporal periodicity of the mode and are called as the Principal Components (PC). Finally the S matrix is a diagonal matrix whose non zero elements are called as the Singular Values (SV) of the mode, they gives information about the energy of the mode. The following identity holds: $X = USV$. From the above identity, it follows that the i^{th} column of U, the i^{th} value of S, and the i^{th} row of V are all related, that is to say that the triplet (PA_i, SV_i, PC_i) describes a given mode. In case of unevenly spaced coils, SVD cannot provide an ideal decomposition between different sinusoidal

modes. Two sinusoidal modes can be present in the same SVD mode. However, the mode with highest energy (the dominant one) will be represented by the triplet associated with the first SV, since SVD' results are ordered from the higher SV to the lower. From the SVD results the characteristics of the mode can be extracted: similarly to [21] the toroidal order number is evaluated by calculating the likelihood L_n of the dominant PA with a theoretical one (Vn) calculated numerically under the assumptions that only a mode with the given periodicity was present: $L_n = L_{1,n}, < PA_1, V_n >^2$. The higher likelihood will indicate the most probable value of n of the dominant mode in the data. A threshold of 0.5 can be taken to discriminate the false positives that can be produced by the noise. The amplitudes of modes with $n = 1, 2, 3, 4, 5$ are calculated by the following expression $A_n = A_x \sum_i SV_i^2 |PA_i \dot{V}_n|^2 / \sum_i SV_i^2$, where A_x is the amplitude of one of the Mirnov coils. The frequency of the dominant mode is calculated as the maximum of the spectrum of the PC.

The main results of the SVD analysis are reported in Fig. 4(c-d) and reveal that a precursor with n=4 mode number, rotating at $70kHz$, is present and it grows exponentially in few tens of ms before the beta collapse. The mode location has been calculated using the mode frequency and the measured radial flow profile calculated from charge exchange recombination spectroscopy data, and it is around $R = 3.48m$, near the $q = 2$ surface. The mode position agrees with the one extimated applying the coherence technique between the pick up coil and ECE fluctuactions, as described in [19]. The radial profile of q is plotted in black in Fig. 4(e) and the q=2 rational surface is marked with squared symbols.

Around t=4.2324s, n=1 activity develops and the temperature profile inside the q=2 surface collapses, as shown in Fig. 4(c)-(e), respectively. Moreover, an inversion radius in temperature measurements is observed, around $R = 3.54m$, as reported in Fig. 4(f). These results suggest that a magnetic field reconnection event, induced by the n=4 mode, which is located around the $q = 2$ magnetic surface, triggers the $n = 1$. The $n = 1$ mode then causes the beta collapse event, as shown in Fig. 4(a).

A statistical analysis, reported in [17], highlights that beta collapse events happen for $\beta_N > 2.5$, value for which the plasma pressure is beyond the no-wall beta limit as suggested by RFA. A detailed characterization of beta collapse events and their effects on plasma performances in ILW plasmas will be presented in a dedicated paper.

The plasma stability limit identified in advanced scenarios on JET-ILW plasmas has been compared with the results obtained during C wall operations when RFA measurements are available. As opposed to C wall plasmas, the RFA technique has been applied in a restricted database of discharges, characterized by q_{min} value around 1.7. In any case, it is possible to compare C wall and ILW results, since RFA measurements in C wall plasmas with $q_{min} \approx 1.7$ are available.

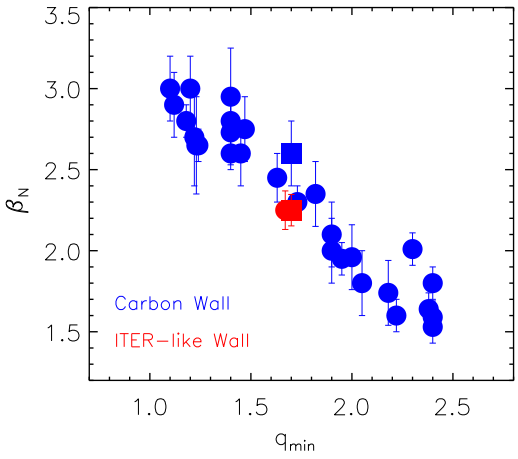

Figure 5: β_N at the time instant when RFA shows a pronounced increase as a function of q_{min}. Each symbol type represents a different pulse. Blue dots correspond to C-wall plasmas, instead red ones to ILW ones.

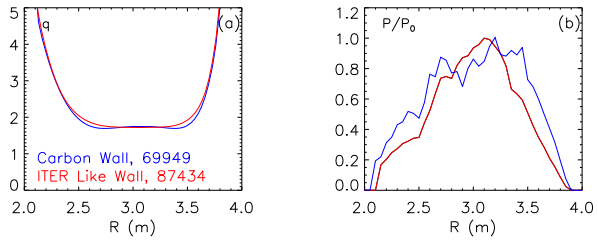

Figure 6: Radial profile of (a) q and (b) normalized plasma pressure for the C wall plasma described in the text, in blue, and ILW one, in red.

The dependence of the β_N, when the RFA increases sharply, on the minimum q is shown in Fig.5. The value of q_{min} has been determined from the EFIT code [18] reconstruction which includes motional Stark effect and low-n MHD activity measurements as constraints. In the figure, different colours correspond to different JET wall plasmas: blue for C wall, red for ILW ones. The decrease of β_N increasing the q_{min} has been already documented in the past, as reported in [11], and it is mainly due to the dependence of plasma stability on the current profile. The new RFA data, collected during ILW experiments, follows the same trend of the C wall ones. More data needs to be collected at different q values in order to confirm the same Carbon wall dependence. Note that, the new RFA data is located in the low part of the trend. Small changes in pressure and current density profiles between C and ILW cases, in particular close to the pedestal region, may cause significant changes in the RWM-driven beta limit [12]. The reason why ILW plasmas reach lower values of β_N with respect to C wall ones has been investigated using the MARS-F code.

The MARS-F code is a linear ideal MHD code which has been used extensively to study the no-wall limit in JET plasmas as documented in [7, 8, 24–26]. The version of the code which takes into account a damping of the perturbed toroidal motion of the plasma due to parallel viscosity has been considered here. A strong sound wave damping coefficient ($k_{||} = 1.5$) has been used, as suggested by a previous study [25].

For the stability analysis, the 87434 plasma at $t = 44.05s$ has been considered. The radial profile of the magnetic equilibrium is reported in red in Fig. 6(a). The plasma stability limit is determined by scanning the plasma pressure while the flux surface averaged toroidal current density profile and the shape of the pressure profile are held constant as a function of poloidal flux. Fig.7(a) summarizes the code stability study results which are indicated with a green dotted line and the experimental data is marked with red dots. Note that the measured pressure limit threshold, around 2.3, agrees reasonably well with the MARS-F code predictions.

The same stability analysis has been carried out for a C wall plasma which has a similar magnetic equilibrium of 87434 experiment, as shown in blue in Fig. 6(a), but reaches an higher β_N value, around 12% with respect to the ILW one. This experiment is marked with a blue square in Fig. 5. The trend of RFA as a function of β_N is reported in Fig. 7(b). The experimental data, marked with blue dots, suggest that the plasma is approaching the beta limit around 2.6. Note that in this experiment, a hysteresis pattern can be observed in the trend RFA as a function of β_N. The time history is highlighted with arrows. Here, the β fall is caused by a reduction of the NBI heating power, instead the decrease of the plasma response is associated with the evolution of the q profile. In the same figure, MARS-F code calculations are reported and are indicated with a green dotted line. Also in this case, the modelled stability limit agrees with the β limit experimentally identified.

The difference in critical β_N between C and ILW plasmas analysed here might be explained by the plasma pressure profile. The radial profiles of plasma pressure are reported in Fig. 6(b). The shape of the pressure profile can be expressed in terms of the pressure peaking factor, defined as $P_0/ < P >$, where P_0 is the pressure on axis and $< P >$ is the volume-averaged pressure. As reported in [27], plasmas with strongly peaked pressure profile, or a high pressure peaking factor, encounter a stability limit at low β_N, while plasmas with broad pressure profiles, or low pressure peaking factor, reach much higher betas.

The C wall plasma has a pressure peaking factor of 1.8, instead the ILW one is around 2.3. This implies that the C wall plasma has a broader pressure profile than the ILW one. The lower beta limit encountered in the ILW experiment therefore is associated with the plasma pressure profile, in agreement with the plasma stability analysis described in [27]. Generally, in ILW plasmas a change of plasma pressure profile has been observed; with respect to C wall profiles an increase of edge pedestal pressure and core pressure peaking, especially at high power, has been obtained [28].

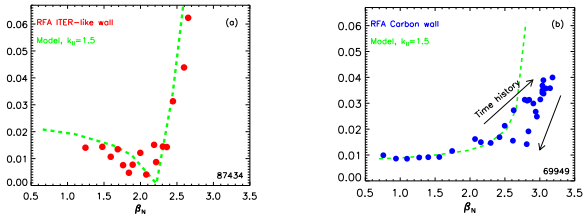

Figure 7: RFA as a function of the normalised plasma pressure of (a) a ILW and (b) a C wall plasma. The dots correspond to experimental data, the dashed green curve to MARS-F code prediction using $k_{||} = 1.5$.

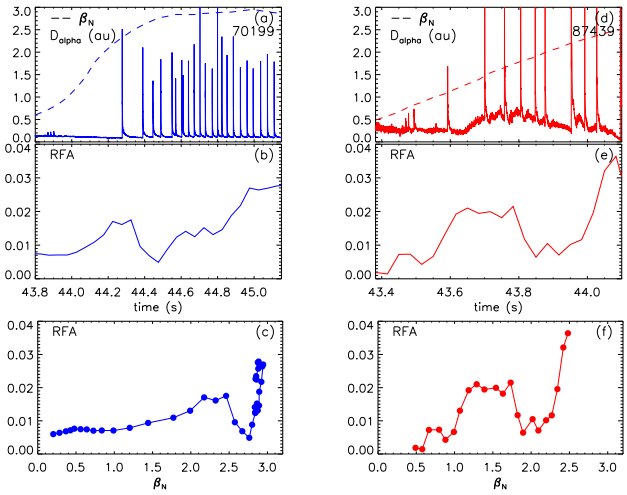

Figure 8: Time behaviour of (a-d) β_N and D_α, (b-e) RFA and (c-f) RFA a function of β_N. The blue data corresponds to a C wall plasma, instead the red ones to ILW experiment.

It is worth mentioning that an increased RFA has been observed at low β_N in some ILW plasmas, as also observed in C wall ones [12, 25]. Figure 8 shows the time behaviour of β_N and D_α signals and RFA for a C wall plasma in panels (a-b) and for a ILW one, in (d-e). The RFA as a function of β_N is reported in Figures 8(c-f). The two RFA peaks occur at β_N values about 2.1 and 1.2, for the C and ILW plasmas, considerably below the estimated no-wall beta limits, which is about 2.8 and 2.3, respectively. Note that, the first ELM in the ILW plasma appears at lower β_N with respect to the C wall one. This is because during ILW operations increased D_2 gas rates are used compared to JET-C ones in order to avoid large impurity influxes of Tungsten into the plasma. The amplification of the plasma response in both cases happens prior to the first ELM, as indicated by D_α measurement, in low pressure regimes. This behaviour is connected with the development of the edge current density during the ELM-free period, which destabilizes the n = 1

ideal peeling mode. Such modes couple with the internal n=1 mode lowering the stability limit, thus increasing the RFA [25].

IV. CONCLUSIONS

In this work, the response of advanced JET-ILW tokamak plasmas to n=1 resonant magnetic field perturbations applied through the EFCCs system has been described and the main results have been compared with the ones obtained during JET-C wall operations. The frequency response of the wall to magnetic field perturbation in absence of plasma has been characterized and the change of the wall from Carbon to a combination of Beryllium and Tungsten has no effects on the magnetic field penetration.

In the presence of plasma, an increase of RFA at low β_N has been observed and this happens before the triggering of the first ELM. Such behavior is similar to previous observations with C wall and it has been explained by the response of marginally stable low n ideal peeling modes which couple with the internal n=1 mode, lowering the plasma stability limit. Note that in ILW plasmas the first ELM appears at lower β_N values than the C ones since increased gas puffing is used to avoid Tungsten contamination.

At higher plasma pressure, beta collapse events have been observed in ILW plasmas and the triggering mechanism is quite different from C wall one: in C wall plasmas the beta collapses were triggered by a global n=1 kink mode which affected all of plasma volume. Instead, in the recent experiments, a global n=1 kink mode is not visible in the magnetics before the events, but in few tens of milliseconds, fast high-n MHD activity develops around the q=2 surface, which triggers the n=1 mode responsible of the beta collapse.

Probably the change of the pressure profile, associated with the presence of heavy impurities [28–30] and the absence of C radiation, is responsible of the different MHD between the ILW and the C wall. A characterization of the MHD precursors before the beta collapse events and the effect of such events on kinetic profiles in ILW plasmas will be described in a separate paper.

In such high plasma pressure regimes, the values of RFA reached in ILW plasmas are compatible with the ones obtained with C wall despite β_N being 12% lower. The MARS-F code has been used to investigate plasma stability and good agreement between the experimental beta-limit detected using the RFA technique and the one predicted by the model has been obtained. The evidence of lower β_N reached in ILW plasmas with respect to the C wall ones has been investigated and it relies on the plasma pressure profile. As predicted by theory [27], plasmas with the same magnetic equilibrium but with peaked pressure profiles are more unstable.

Generally, more RFA measurements need to be collected in future ILW experiments in order to compare the plasma stability limit in a wide range of magnetic equilibria. On the modelling side, computing the self-consistent drift kinetic response [31] of the high β plasmas in JET device remains as future work.

V. ACKNOWLEDGMENTS

This work has been carried out within the framework of the EUROfusion Consortium and has received funding from the EURATOM research and training programme 2014-2018 under grant agreement No 633053 and from the RCUK Energy Programme (grant number EP/I501045). To obtain further information on the data and models underlying this paper please contact PublicationsManager@ccfe.ac.uk. The views and opinions expressed herein do not necessarily reflect those of the European Commission.

[1] Taylor T. S. 1997 *Plasma Phys. Control. Fusion* **39** B47
[2] Chu M. S. and Okabayashi M. 2010 *Plasma Phys. Controlled Fusion* **52** 123001
[3] Troyon F. et al 1984 *Plasma Phys. Controlled Fusion* **26** 209
[4] Garofalo A.M. et al 2003 *Phys. Plasmas* **10** 4776
[5] Strait E.J. et al 2003 *Nucl. Fusion* **43** 430
[6] Reimerdes H. et al 2004 *Phys. Rev. Lett.* **93** 135002
[7] Hender T.C. et al 2004 Resistive wall mode studies in JET Proc. 20th IAEA Fusion Energy Conf. 2004 (Vilamoura, Portugal, 2004) (Vienna: IAEA) IAEA-CN-116/ EX/P2-22 CD-ROM file EX/P2-22
[8] Hender T.C. et al 2006 Prediction of Rotational Stabilisation of ResistiveWall Modes in ITER Proc. 21st IAEA Fusion Energy Conf. 2006 (Chengdu, China, 2006) (Vienna: IAEA) IAEACN- 149/ EX/P8-18 CD-ROM file EX/P8-18
[9] Chapman I.T. et al 2009 *Plasma Phys. Control. Fusion* **51** 055015
[10] Reimerdes H. et al 2005 *Nucl. Fusion* **45** 368
[11] Gryaznevich M.P. et al 2008 *Plasma Phys. Control. Fusion* **50** 124030
[12] Gryaznevich M.P. et al 2012 *Nucl. Fusion* **52** 083018
[13] Igochine V. et al 2013 Identification of the beta lomit in ASDEX Upgrade Proc. 40nd EPS Conference on Plasma Physics 1 - 5 July 2013. Helsinki, Finland
[14] Gregoratto D. et al 2005 *Phys. Plasmas* **7** 12 092510
[15] Liu Y.Q. et al 2000 *Phys. Plasmas* **7** 3681
[16] Barlow I. et al 2001 *Fusion Eng. Des.* **58-59** 189
[17] Alessi E. et al 2015 MHD Analysis of Beta Collapses in AT JET Discharges Proc. 42nd EPS Conference on Plasma Physics 22 - 26 June 2015. Lisbon, Portugal
[18] Lao L. et al 1985 *Nucl. Fusion* **25** 1611
[19] Baruzzo M. et al 2010 *Plasma Phys. Control. Fusion* **52**

075001
[20] Nardone C. et al 1992 *Plasma Phys. Control. Fusion* **34** 1447
[21] Galperti C. et al 2014 *Plasma Phys. Control. Fusion* **56** 114012
[22] Buratti P. et al 2012 *Nucl. Fusion* **52** 023006
[23] Baranov Yu F. et al 2012 *Nucl. Fusion* **52** 023018
[24] Liu Y.Q. et al 2006 *Phys. Plasmas* **13** 056120
[25] Liu Y.Q. et al 2009 *Plasma Phys. Control. Fusion* **51** 115005
[26] Liu Y.Q. et al 2010 *Plasma Phys. Control. Fusion* **52** 045011
[27] Bondenson A. et al 1999 *Nucl. Fusion* **39** 1523
[28] Challis C.D. et al 2015 *Nucl. Fusion* **55** 053031
[29] Maggi C.F. et al 2015 *Nucl. Fusion* **55** 113031
[30] Beurskens M. et al 2013 *Plasma Phys. Control. Fusion* **55** 124043
[31] Wang Z. et al 2015 *Phys. Rev. Lett.* **114** 145005